

# A silicon strip detector system for high resolution particle tracking in turbulence

Greg A. Voth, Arthur La Porta, and Alice M. Crawford

*Laboratory of Atomic and Solid State Physics, Cornell University, Ithaca, New York 14853-2501*

Eberhard Bodenschatz<sup>a)</sup>

*Laboratory of Atomic and Solid State Physics, Cornell University, Ithaca, New York 14853-2501*

Curt Ward and Jim Alexander<sup>b)</sup>

*Laboratory of Nuclear Studies, Cornell University, Ithaca, New York 14853-2501*

(Received 10 July 2001; accepted for publication 12 September 2001)

We describe a high speed imaging system that is used to track tracer particles in highly turbulent flows. The system uses silicon strip detectors designed for high energy physics experiments and is capable of reading two detectors at a frame rate of 70 kHz. Each detector contains 512 strips and measures a one-dimensional projection of the light striking it. The position measurements from this system have a dynamic range of 6400:1. Extensions to higher frame rates and more detectors are possible. We describe the detectors, readout system, supporting systems, and give an evaluation of the measurement accuracy. © 2001 American Institute of Physics. [DOI: 10.1063/1.1416112]

## I. INTRODUCTION

A long standing problem in turbulence research has been the difficulty of making accurate experimental measurements of particle trajectories in a highly turbulent flow.<sup>1</sup> Optical imaging has been the standard approach to this problem, but commercially available imaging systems have had limited success even with the current revolution in electronic imaging technology. A reason for this is revealed in Fig. 1, which shows measured three-dimensional trajectories of four particles in a high Reynolds number turbulent water flow. The particles' acceleration changes by many times the rms acceleration in 40 ms. We find that in order to adequately resolve the acceleration probability distribution from trajectories such as these we need greater than 50 000 positions per second while maintaining very high spatial resolution. Standard charge coupled device (CCD) based video systems cannot meet these requirements because of the huge data rates involved.

However, consideration of the contents of typical particle tracking images from CCD systems suggests a solution to the data rate problem. The images are mostly zeros with a few bright pixels marking particle positions. When the number of particles in view is small, the information can be much more efficiently represented by two orthogonal one-dimensional (1D) projections rather than by a two-dimensional (2D) image.

We have implemented an imaging system based on silicon strip detectors that is able to record the data from two projection imagers at 70 000 frames per second. Although these detectors were specifically designed for use in vertex detectors for high energy physics experiments, they also function efficiently as optical imaging elements. They consist

of 512 charge sensitive strips with individual integrated low noise preamplifiers, and so measure the 1D projection of the light striking the detector. The large imaging rate is possible since only 512 strips must be read out compared with  $512 \times 512$  pixels for a CCD of similar spatial resolution. With these detectors we have obtained tracer particle positioning accuracy of 0.08 pixels, or 0.6  $\mu\text{m}$  in the flow. Detailed descriptions of results obtained with this particle tracking system are in Refs. 2 and 3.

## II. RELATED MEASUREMENT TECHNIQUES

Most previous particle tracking measurement systems have been limited to flows with slow time scales, which for laboratory flows means low Reynolds numbers. Pioneering studies used a series of film cameras,<sup>4</sup> and later a single CCD imager.<sup>5</sup> Recently an approach using four CCD cameras to image a subvolume of the flow from different angles has been developed.<sup>6,7</sup> This allows the three-dimensional (3D) positions of particles to be reconstructed by matching the images from the four cameras. Up to  $10^3$  particles can be tracked simultaneously using this technique, but the large amount of data per image has limited frame rates to 25 Hz. At significant expense, CCD systems can be obtained that extend this frame rate to about 1 kHz at 512 pixel spatial resolution. However, this is still more than an order of magnitude too slow to measure accelerations along the trajectory in Fig. 1. In addition, strip detector systems scale to higher spatial resolution more easily since they only require  $N$  rather than  $N^2$  samples per image.

One device that has even higher temporal resolution than strip detectors is the position sensitive photodiode. These devices output analog signals from which the average position of the light striking them can be calculated. As a result, they give spurious readings when multiple particles are in view. They have been used to make acceleration measurements in turbulence<sup>8</sup> but their spatial resolution and light

<sup>a)</sup>Electronic mail: ebzz@cornell.edu

<sup>b)</sup>Electronic mail: jima@lms.cornell.edu

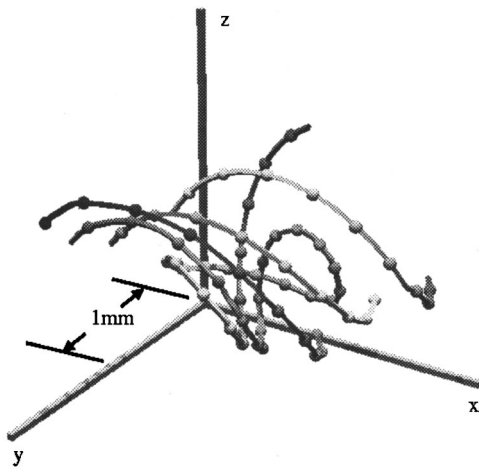


FIG. 1. Three-dimensional time resolved trajectories of four particles caught in an intense vortex structure. The spherical markers are equally spaced in time with 8 frames (0.11 ms) between them. This data was taken with two detectors: two position coordinates are measured by primary signals and the third coordinate is measured by both conjugate signals. Some manual control was necessary to accurately match tracks when four particles with conjugate signals were in view. Accelerations in these rare events are regularly greater than  $10\,000\text{ m/s}^2$ .

sensitivity are often not adequate even when only one particle is in view. A similar device, the position sensitive photomultiplier, has extremely high light sensitivity and time resolution but has even lower spatial resolution than position sensitive photodiodes.

Recently, ultrasonic doppler velocimetry has been developed to measure Lagrangian velocity fluctuations in turbulent flows.<sup>9</sup> This has allowed accurate measurement of particle velocities over long times. Another approach that shows promise is holographic particle tracking.<sup>10</sup> This method allows full 3D particle displacements to be measured from a single image. Currently the slow process of interrogating film holograms limits its use to a few frames.

### III. SILICON STRIP DETECTORS

Silicon strip detectors have been developed for use in vertex detectors for high energy colliding beam experiments. In these applications hundreds of strip detectors are arrayed in cylindrical shells around the beam interaction point to measure the trajectories of the charged products of subatomic particle decays. The strip detectors we use were designed for the CLEO III experiment at the Cornell electron-positron collider.<sup>11</sup> They are essentially large ( $5.12 \times 2.56\text{ cm}^2$ ) planar photodiodes, made of  $300\text{ }\mu\text{m}$  thick high resistivity *n*-doped silicon. The front, junction side is subdivided by *p*-type implants into 512 sense strips. Measurement of the photocurrent in each of the strips provides a 1D projection of the light striking the detector. Figure 2 shows a photograph of a detector with its front-end readout electronics.

To provide 2D position measurements for the high energy physics experiments, the back (ohmic) side of the detectors is also divided by *p*-type barriers into 512 *n*-type sense strips orthogonal to the front strips. Unfortunately, we find that the signal from the back side is very weak when detecting the visible photons used in the turbulence experi-

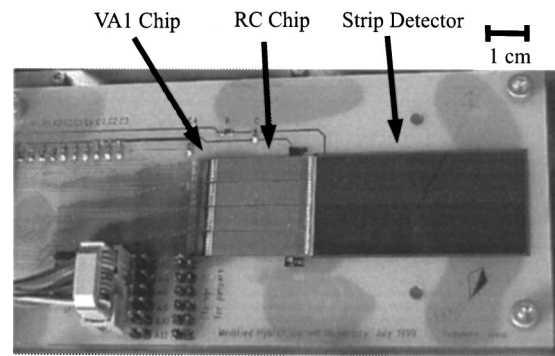


FIG. 2. Photograph of a silicon strip detector mounted with front-end readout electronics. Wirebonds connect each strip between the detector, RC, and VA1 chips. The ribbon cable in the lower left carries the four differential analog output lines.

ments. Our interpretation is that since visible photons are absorbed in a shallow surface layer in the detector, many of the electrons are trapped in surface states and do not migrate immediately to the back side. As a result we use only the front side of the detector for our primary measurements, with each detector measuring one position coordinate. Since only the front side is required, simpler single sided detectors can be used.

Despite the weak signals to the back side of the detector, there is still a way to obtain both coordinates from a single detector. This relies on the particular layout of the detectors we use, as shown in Fig. 3. Because of the geometry of the detector array in the high energy experiments, the front of the detector has readout traces that run perpendicular to the front sense strips. When visible photons are absorbed in the detector the holes migrate to the nearby sense strips, but electrons that are trapped in surface states capacitively couple to the nearby readout traces. This produces a negative signal from which the second position coordinate can be measured. This conjugate signal is weaker than the primary signal and often is not used. However, it can be useful for measuring an additional spatial coordinate and for deciphering trajectories of complex events involving multiple particles. An example is Fig. 1, in which 3D trajectories are obtained from two detectors. This uses each primary signal to measure one coordinate, and the conjugate signals to measure the third. When the conjugate signal is not needed we can eliminate it by adjusting the detector bias voltage.

We have tested detectors from three different fabrication runs of the CLEO III detectors: a prototype made by CSEM

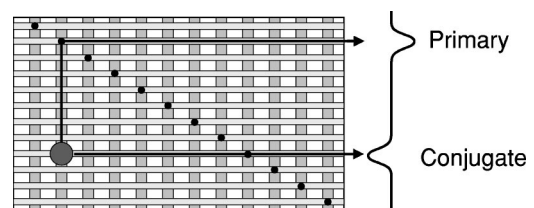


FIG. 3. Diagram of charge collection on the front side of a strip detector. Dark vertical bars designate *p*-type sense strips. Lighter horizontal strips designate aluminum readout traces. The primary signal current is created by direct readout of holes. The conjugate current is from capacitive coupling of photoelectrons to the readout traces.

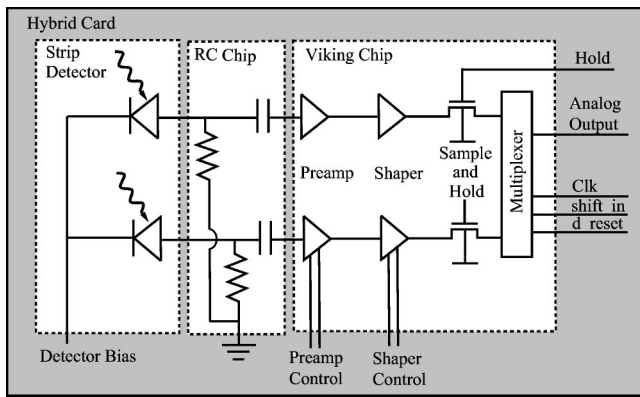


FIG. 4. Schematic of two strips of the detector and front-end readout electronics. The detector bias voltage is typically 100 V. The leads to the VA1 (Viking) chip include the preamp and shaper control signals along with the timing and analog output signals.

Corporation,<sup>12</sup> a prototype by Hamamatsu, and the final production detectors by Hamamatsu.<sup>13</sup> The Hamamatsu detectors are found to have a factor of 5 better efficiency for detecting 500 nm photons than the CSEM detectors. This was somewhat surprising since the detectors have comparable efficiency in detecting minimally ionizing radiation. It is likely that different production techniques resulted in different characteristics of the surface states, which strongly affect collection of charge liberated near the surface. The characteristics of the capacitance versus bias voltage curves for the CSEM detectors also support the interface state theory. A change in the surface states would have a much larger effect on the detection of visible photons absorbed near the surface than on radiation which liberated charge throughout the bulk of the detector.

## IV. DETECTOR READOUT SYSTEM

### A. Front-end electronics

A diagram showing two strips of the detector and front-end readout electronics is shown in Fig. 4. A positive voltage of approximately 100 V is applied to the back side of the detector to fully deplete it. Each strip on the detector is capacitively coupled to an individual integrated low noise amplifier. After a signal passes through the shaper, the sample and hold stores it for the output multiplexer.

The detector and front-end electronics are all mounted on a small printed circuit board, as shown in Fig. 2. These boards were specially printed for the parallel readout required by the turbulence experiment. The front-end electronics are contained on two kinds of silicon chips. The bias resistors (20 M $\Omega$ ) and coupling capacitors (120 pF) are on a chip custom designed for the CLEO experiment (RC chip). The amplifier through the multiplexer are contained in an integrated circuit, the VA1 from IDE AS Co.<sup>14,15</sup> Each RC and VA1 chip supports 128 sense strips, so there are four of each of them connected to a 512 strip detector. Detector fabrication involves mounting all the chips on the circuit board and then attaching the 1024 wirebonds to connect each strip to its RC channel and then to the VA1. Typically about 5% of the strips on a completed detector are dead as a result of

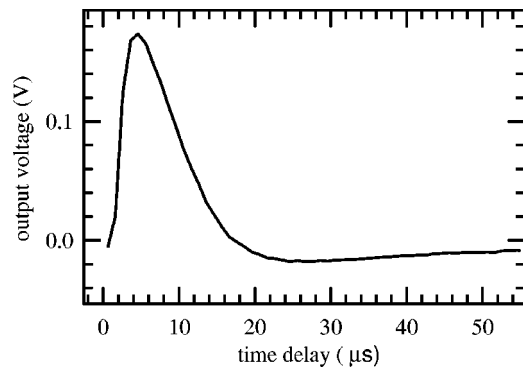


FIG. 5. Shaper output voltage as a function of the time delay between an approximately  $\delta$  function light pulse and the sample time.

defective RC or VA1 chip channels, wirebonding problems, or sense strips with large leakage current. Detector fabrication is accomplished using the clean room and wirebonding equipment that had been installed at Cornell for fabrication of the CLEO III detectors.

The front-end electronics use ac coupling and a shaper because they were designed for detection of high energy particles which deposit their charge in nearly a  $\delta$  function pulse. In the turbulence experiments the laser illumination is pulsed to provide similar charge injection. Optimal detector sensitivity is obtained by adjusting the duration and timing of the illumination pulse and the parameters that control the shaper response function. Figure 5 shows the shaper output voltage created in response to 1  $\mu$ s light pulses, as a function of the time between the light pulse and the sample time. This gives a good approximation of the  $\delta$  function response of the detector. The output resulting from longer illumination times can be obtained from the convolution of this function with the intensity wave form.

### B. Detector control and data processing

Up to this point the system is quite similar to the design used in high energy physics experiments. However, the digitization and data storage systems required significant modifications to allow high speed readout. Figure 6 shows a block diagram of the detector readout system.

The multiplexer in each VA1 outputs a serial analog voltage which encodes the intensity on each of 128 strips. The four VA1 multiplexers are each clocked at 10 MHz. After amplification the output is digitized by 12 bit analog-to-digital converters housed in Pentium Pro computers. The A/D converters are from GaGe Applied Sciences (CompuScope 6012/PCI with X1 external clock).<sup>16</sup> Each PC contains 2 A/D cards which each have two channels, so one PC can read out one strip detector. The GaGe cards each have 1 MB memory buffers, which allows up to 4000 sequential frames to be acquired from a strip detector. After the data is downloaded to main memory over the PCI bus, the cards are enabled to allow concurrent acquisition and processing.

Online processing begins with subtraction of the pedestal, which is the voltage offset from each of the preamplifiers. The 12 bit A/D converters are required to maintain at least 8 bits of dynamic range, since the pedestals are larger

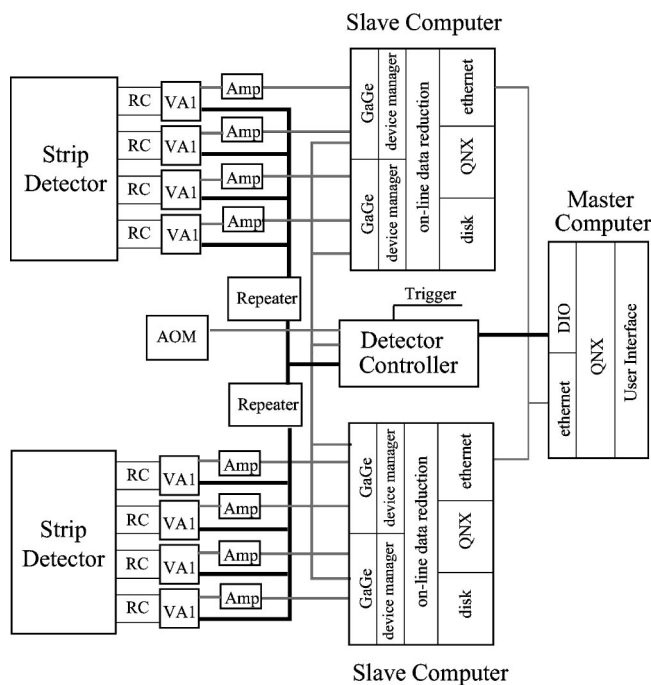


FIG. 6. Block diagram of the readout electronics. The analog output from the VA1 chips is amplified and then digitized in the slave computers. The detector controller and master computer synchronize and mediate readout. Repeater cards convert signals to low voltage for the VA1 chips. The acousto-optic modulator (AOM) is used to modulate the laser intensity at the readout frequency.

than typical signals. A common mode correction is applied to each frame. This removes low frequency noise by subtracting the mean of all strips that do not have a significant signal on them. The computers then compress the data by thresholding before writing it to disk. We use a two level flag tree system for packing the compressed data.

The signals to control and synchronize readout of the detectors are produced by the detector controller.<sup>17</sup> This is a custom-built digital circuit based on an Altera programmable array logic unit. Repeater cards convert the transistor-transistor logic signals from the detector controller into low voltage levels used by the VA1 chips. They also control the preamplifier and shaper settings. We used spare repeater cards that had been fabricated for high energy physics experiments.

Overall control of the system lies with the master computer. It runs the user interface software and mediates the acquisition process to ensure that all components are ready when image acquisition is initiated. A significant consideration in the design of this readout system was the ease of scaling up the system to read more detectors. Since readout is centrally controlled and fully parallel, more detectors can be accommodated by simply adding more slave computers with A/D converters.

One of the major investments in developing this system was the software necessary for detector readout. The computers all run QNX, a realtime operating system with efficient message passing utilities for multinode systems such as this. This provides excellent control of the timing of data acquisition and storage, but requires custom software.

The maximum effective frame rate is 69.9 kHz. Since

each A/D converter runs at 10 MHz and reads 128 strips per frame, the theoretical maximum frame rate is 78.1 kHz, but a brief delay is required before the VA1 chip can rearm itself for acquisition. The frame rate is selectable in the range 5–69.9 kHz. Acquisition of 4000 frames takes 800 ms at the lowest frame rate and 57 ms at the maximum frame rate. The time required to process and store one sequence of frames is approximately 1 s. The 10 MHz clock speed is not a fundamental limit of any system components. It was chosen as a frequency which met the requirements of the turbulence measurements and did not create undo problems driving the signals over the 1–3 m cables that are required by the setup. By upgrading line drivers in the detector controller and minimizing distance between components, it is likely that the readout rates could be increased by a factor of 2 without a major increase in measurement noise.

A typical data run entails acquisition of 50 000 sequences, each containing 4000 images from each of the two detectors. A single image contains 12 bit intensities from 512 strips. Uncompressed, this would be 300 gigabytes, but since only a few strips in each image contain particles, this compresses to about 2 gigabytes. Since a sequence is acquired in about 1 s, a typical data run lasts 14 h. The largest runs contained 150 000 sequences and lasted 42 h.

Postacquisition analysis involves identifying particle positions from the images and then combining the images from different detectors into particle trajectories (for details see Ref. 3). This is achieved by first joining particle positions measured from a single detector to give one coordinate of the trajectory. Although this is fairly simple in principle, care is required when two particles cross or when trajectories involve dead pixels. The 1D trajectories are then matched with the trajectories from the other detectors. (Currently there are two detectors, but when the conjugate signals are used this produces four 1D trajectories.) Matching trajectories between detectors is simple when there is only one particle in view. Correctly matching when multiple particles are in view requires the use of the correlation of intensity measured on different detectors. We find that the intensity is highly correlated between two detectors that use a beam splitter to view the same image. Matching data from detectors that use a different viewing angle requires that one position coordinate be repeated.

## V. SUPPORTING SYSTEMS

Measurement of particle trajectories in turbulence requires integration of the strip detectors with a turbulent flow and systems to provide illumination and optical imaging onto the detector. Figure 7 shows a schematic of the turbulent flow and optical system. Details of the setup are available in Refs. 2, 3, and 17, so here we provide only an overview necessary to understand the capabilities of the strip detector system. The flow we performed measurements on is a turbulent water flow between counter-rotating disks. This produces large Reynolds numbers while still allowing the optical system to be within 33 cm of the center of the flow. For tracer particles we typically use 46  $\mu\text{m}$  polystyrene spheres.

The illumination is provided by a multiline argon ion

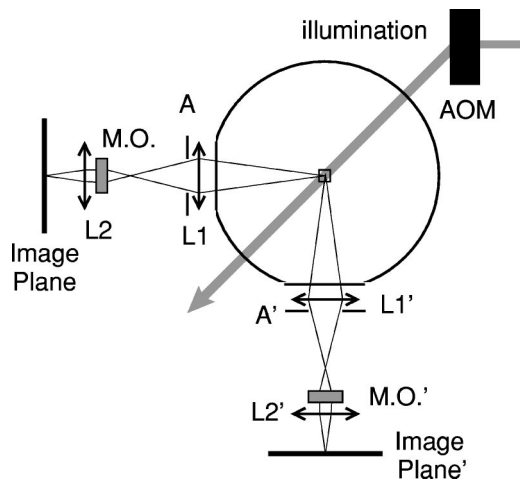


FIG. 7. Illumination and optical imaging system. The volume illuminated by the laser is imaged by two optical systems at  $45^\circ$  forward scattering. L1 and L2 are doublet lenses, A is an aperture, and MO is a microscope objective. The detector at the image plane can be rotated to measure either of two position coordinates. It is also possible to have two detectors measure the two position coordinates from a single optical axis by placing a beam splitter between MO and L2.

laser beam that is pulsed with an acousto-optic modulator. The pulsed illumination is required because the detectors are ac coupled. For future experiments, the illumination laser will be upgraded to a  $Q$ -switched Nd-YAG in order to provide more light and to make optimal use of the shaper response. For acceleration measurements we typically illuminate a volume in the center of the flow with a 2 mm diameter cylindrical beam. The imaging axis is  $45^\circ$  from the beam propagation direction to take advantage of the larger intensity in forward scattering. A set of lenses then image  $10 \text{ mm}^3$  of the illuminated volume onto the detectors. The optics must have large depth of field to keep the full detection volume in focus. This typically requires a numerical aperture of less than 0.03, which allows small diameter, inexpensive optics to be used. The optics can be configured with a beamsplitter to allow two detectors to measure different position coordinates from the same viewing angle.

Calibration and focusing pose special challenges for a 1D ac coupled imaging system. We have worked with the Cornell Nanofabrication Center to produce calibration masks for this purpose. These are standard masks for optical lithography that have a line of dots etched in the reflective coating. These are placed in the fluid chamber filled with water, and the pulsed laser beam illuminates an opal glass diffuser placed directly behind the mask. In addition to calibration, this also allows rough focusing of the optics. Fine focusing is performed by measuring a series of particle tracks and adjusting the focus until the spots in the center of the field of view have the smallest diameter.

## VI. SAMPLE DATA AND MEASUREMENT ACCURACY

Figure 8 shows an example of a particle trajectory recorded with one strip detector. The top grayscale plot shows the raw data recorded by the data acquisition system. Background gray areas were not stored by the compression algorithm. Other areas show the signal voltage on that strip in

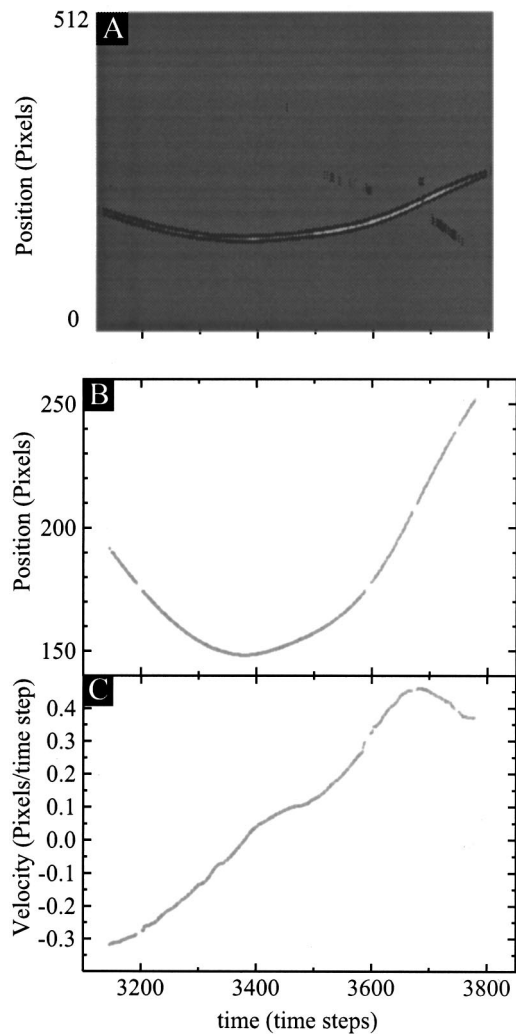


FIG. 8. Example of a trajectory measured by the strip detector. 512 pixels corresponds to 3.88 mm in the flow. The readout period is  $14.3 \mu\text{s}$ , which is a frequency of 69 930 Hz.

grayscale. The position data which was measured from this track is shown in Fig. 8(b). Velocities calculated from linear fits to 15 time steps are shown in Fig. 8(c).

The typical intensities along the trajectory in Fig. 8(a) are approximately 50 mV compared to the detector noise floor of 0.5 mV. This corresponds to a signal charge of 10 000 electrons and 100 electrons noise.

The position measurement error can be estimated by the rms deviations of the measured position from a fit to the trajectory. Figure 9 shows the position measurement error as a function of the maximum intensity of the trajectory in that frame. In this case the fit used to determine the error was a quadratic polynomial fit to 33 time steps [ $0.5\tau_\eta$  where  $\tau_\eta = (\nu/\epsilon)^{1/2}$  is the Kolmogorov time]. For the brightest trajectories the position error is less than 0.05 pixels which corresponds to  $0.4 \mu\text{m}$  in the flow. Position measurement errors in this range are common for CCD imaging systems, for example, Ref. 7 reports measurement errors in the range 0.02 to 0.1 pixels. The typical rms position measurement error for the entire sample depends on how bright particles must be before they are included in the sample. For the intensity threshold we used (8 mV), the rms measurement error aver-

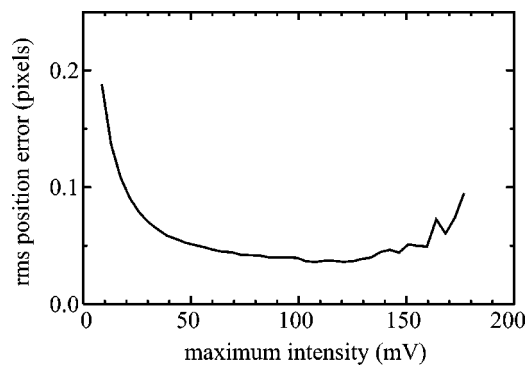


FIG. 9. Position measurement errors as a function of the peak intensity of a particle image. The saturation effects seen at very rare high intensity are not significant since they represent only a small number of particles. Using an intensity threshold of 8 mV, the rms measurement error averaged over all intensities is found to be 0.08 pixels.

aged over all intensities was 0.08 pixels, or  $0.6 \mu\text{m}$  in the flow.

## VII. DISCUSSION

Silicon strip detectors provide an excellent tool for high speed measurement of particle trajectories in turbulence. We have implemented a system that reads out two detectors at 70 000 frames per second. Two more detectors are currently being installed to allow high resolution 3D measurement. This detection system has opened a new window on the study of particle motion in turbulence. It is likely that similar systems could be useful for other sparse imaging applications that require high spatial resolution and very high frame rates.

## ACKNOWLEDGMENTS

The authors thank Pablo Hopman for assistance in detector fabrication. This research was supported by the National Science Foundation.

- <sup>1</sup>B. Sawford, *Annu. Rev. Fluid Mech.* **33**, 289 (2001).
- <sup>2</sup>A. La Porta, G. A. Voth, A. M. Crawford, J. Alexander, and E. Bodenschatz, *Nature (London)* **409**, 1017 (2001).
- <sup>3</sup>G. A. Voth, A. La Porta, A. M. Crawford, J. Alexander, and E. Bodenschatz (unpublished) (2001).
- <sup>4</sup>W. H. Snyder and J. L. Lumley, *J. Fluid Mech.* **48**, 41 (1971).
- <sup>5</sup>Y. Sato and K. Yamamoto, *J. Fluid Mech.* **175**, 183 (1987).
- <sup>6</sup>T. Dracos, *Three-Dimensional Velocity and Vorticity Measuring and Image Analysis Techniques* (Kluwer, Dordrecht, 1996).
- <sup>7</sup>S. Ott and J. Mann, *J. Fluid Mech.* **422**, 202 (2000).
- <sup>8</sup>G. A. Voth, K. Satyanarayan, and E. Bodenschatz, *Phys. Fluids* **10**, 2268 (1998).
- <sup>9</sup>N. Mordant, P. Metz, O. Michel, and J.-F. Pinton (unpublished).
- <sup>10</sup>B. Tau, J. Katz, and C. Meneveau, *Phys. Fluids* **12**, 941 (2000).
- <sup>11</sup>J. Fast *et al.*, *Nucl. Instrum. Methods Phys. Res. A* **435**, 9 (1999).
- <sup>12</sup>CSEM Corporation, Rue Jaquet-Droz 1, P.O. Box CH-2007, Neuchatel, Switzerland, [www.csem.ch](http://www.csem.ch)
- <sup>13</sup>Hamamatsu Photonics KK, 325-6 Sunayama-cho, Hamamatsu City, Shizuoka Pref, 430-8587, Japan, [www.hamamatsu.com](http://www.hamamatsu.com)
- <sup>14</sup>O. Toker, S. Masciocchi, E. Nygård, A. Rudge, and P. Weillhammer, *Nucl. Instrum. Methods Phys. Res. A* **340**, 572 (1994).
- <sup>15</sup>IDEAS Co., Veritasueien 9, Box 315 N-1323, Hovik, Norway, [www.ideas.no](http://www.ideas.no)
- <sup>16</sup>GaGe Applied, 2000 32nd Avenue, Lachine, QC Canada H8T 3HL, [www.gage-applied.com](http://www.gage-applied.com)
- <sup>17</sup>G. Voth, Ph.D. thesis, Cornell University, 2000.